BIOCHEMISTRY
including biophysical chemistry & molecular biology

ARTICLE

pubs.acs.org/biochemistry

The Ribotoxin Restrictocin Recognizes Its RNA Substrate by Selective Engagement of Active Site Residues

Matthew J. Plantinga,[‡,§,▽] Alexei V. Korennykh,[⊥,#] Joseph A. Piccirilli,[*,‡,⊥] and Carl C. Correll[*,∥,‡,§]

[‡]Department of Biochemistry and Molecular Biology, and [⊥]Department of Chemistry, The University of Chicago, Chicago, Illinois 60637

[§]Department of Biochemistry and Molecular Biology, Rosalind Franklin University of Medicine & Science, North Chicago, Illinois 60064

ABSTRACT: Restrictocin and related fungal endoribonucleases from the α-sarcin family site-specifically cleave the sarcin/ricin loop (SRL) on the ribosome to inhibit translation and ultimately trigger cell death. Previous studies showed that the SRL folds into a bulged-G motif and tetraloop, with restrictocin achieving a specificity of ∼1000-fold by recognizing both motifs only after the initial binding step. Here, we identify contacts within the protein−RNA interface and determine the extent to which each one contributes to enzyme specificity by examining the effect of protein mutations on the cleavage of the SRL substrate compared to a variety of other RNA substrates. As with other biomolecular interfaces, only a subset of contacts contributes to specificity. One contact of this subset is critical, with the H49A mutation resulting in quantitative loss of specificity. Maximum catalytic activity occurs when both motifs of the SRL are present, with the major contribution involving the bulged-G motif recognized by three lysine residues located adjacent to the active site: K110, K111, and K113. Our findings support a kinetic proofreading mechanism in which the active site residues H49 and, to a lesser extent, Y47 make greater catalytic contributions to SRL cleavage than to suboptimal substrates. This systematic and quantitative analysis begins to elucidate the principles governing RNA recognition by a site-specific endonuclease and may thus serve as a mechanistic model for investigating other RNA modifying enzymes.

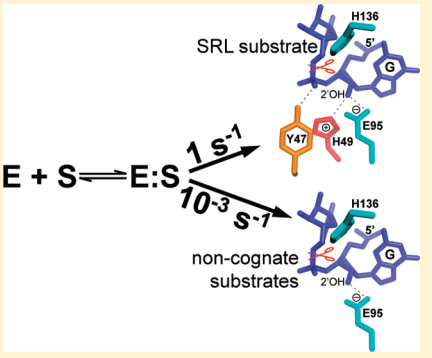

Site-specific modification of folded RNA by enzymes is common to many biological processes. The molecular bases of these processes are not understood sufficiently because of the dual requirements for structural analyses that identify candidate surface contacts and for solution studies that quantitatively evaluate their contribution to site-specific cleavage. The site-specific ribotoxin restrictocin is a suitable candidate for such studies because it is well characterized both structurally[1,2] and kinetically.[3,4]

Restrictocin and related fungal ribotoxins such as α-sarcin are small endoribonucleases that cleave one site in the conserved sarcin/ricin loop (SRL) in 23S-28S rRNA to disrupt GTPase activation when elongation factors bind to the ribosome,[5] halt protein synthesis, and ultimately trigger apoptotic cell death (reviewed in refs 6 and 7). Ribotoxins share the same fold and catalytic mechanism as the well-studied T1 endoribonuclease family of fungal enzymes.[1,8,9] In these enzymes, in-line attack of a nucleophilic 2′-hydroxyl group on the 3′ adjacent phosphate produces a 5′-hydoxyl group and a 2′,3′-cyclic phosphate[3,4] (Figure 1). Despite these similarities, substrate specificity differs greatly. T1 enzymes cleave on the 3′-side of every G nucleotide in single-stranded RNA. In contrast, ribotoxins recognize a single-folded RNA structure on the ribosomal surface, the SRL, and specifically cleave a single phosphodiester bond within the SRL tetraloop. For structural and functional studies, including those described herein, a minimal substrate is used in which the ribosome is trimmed to the ∼30 nucleotides of the SRL sequence, designated the SRL substrate.[7,10] This minimal substrate is sufficient to replicate the site-cleavage observed in the SRL embedded in the ribosome.[11] Moreover, restrictocin catalyzes the cleavage of this minimal substrate and the ribosome with the same k_{cat} value.[3]

Structural studies identified distinctive features in the SRL RNA that contribute to site-recognition by ribotoxins. The loop portion of the SRL stem-loop structure folds into two motifs: a GAGA tetraloop and a bulged-G motif[12−16] (Figure 1). Both motifs contribute to ribotoxin recognition,[4,17] with cleavage occurring between the third and the fourth nucleotide of the tetraloop (Figure 2). To identify the enzyme substrate interface, co-crystal structures were determined for restrictocin bound to several different substrate analogues.[2] These structures provide the basis for a model that involves simultaneous docking of the protein to both SRL motifs (Materials and Methods and Figure 1C,D). A loop containing K110, K111, and K113, designated the lysine triad, recognizes the bulged-G nucleobase of the eponymous motif and the enlarged major groove of the SRL. A β-sheet surface recognizes a base flipped form of the target nucleotide (the second G of the GAGA tetraloop) that places it in the active site with an in-line orientation poised for cleavage.

Received: November 16, 2010
Revised: March 2, 2011
Published: March 18, 2011

dx.doi.org/10.1021/bi1018336 | *Biochemistry* 2011, 50, 3004–3013

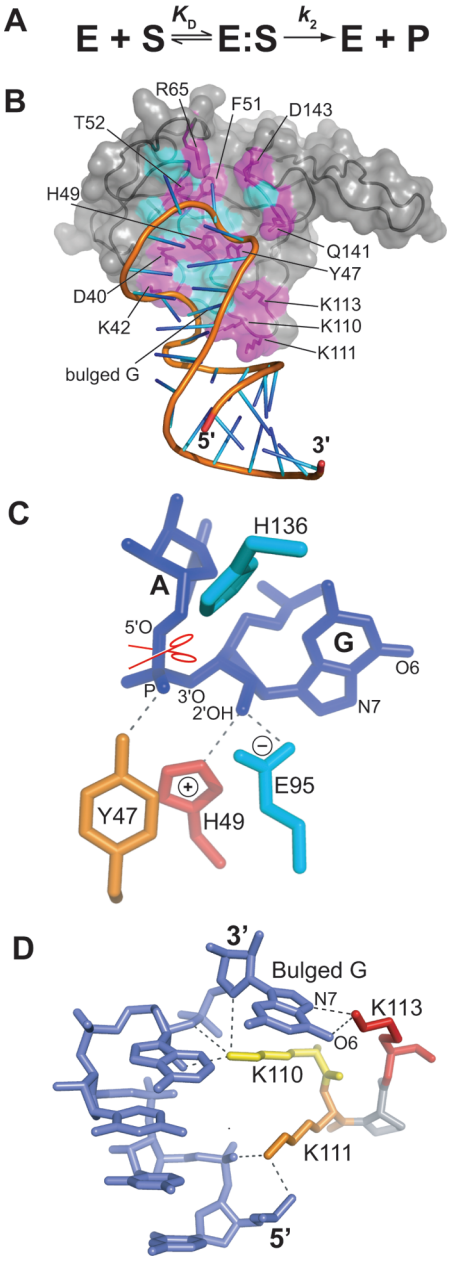

Figure 1. Kinetic and structural models for SRL substrate recognition and cleavage by restrictocin. (A) Reaction scheme for restrictocin (E) and its substrate the SRL (S). The single-turnover kinetic parameter $K_{1/2}$ monitors initial binding to form the E:S complex and equals K_D and K_m. The unimolecular rate constant k_2 monitors subsequent conversion of the E:S complex to products and free enzyme. (B) Model of a restrictocin−SRL complex docked for site-recognition.[2] Colored protein residues on the surface of restrictocin highlight protein side-chain contacts mutated in this study (magenta; residues labeled) and protein backbone contacts not mutated in this study (unlabeled teal residues are G41, T43, G44, S46, W50, N53, G54, I62, E95, and G142). (C) Close-up view of the restrictocin active site, showing a docked G nucleotide. Structural and biochemical studies[9] offer evidence that E95 serves as a general base and H136 as a general acid; H49 may assist E95 in deprotonating the 2′OH nucleophile. Scissors mark the scissile bond. (D) Interactions between the lysine triad (K110, K111, and K113) and the bulged-G motif. Dotted lines show protein−RNA hydrogen bonds.

From the RNA side of the enzyme−substrate interface, mutations in the tetraloop and stem are tolerated. In contrast, mutations of the bulged-G nucleobase to A, C, or U abolished

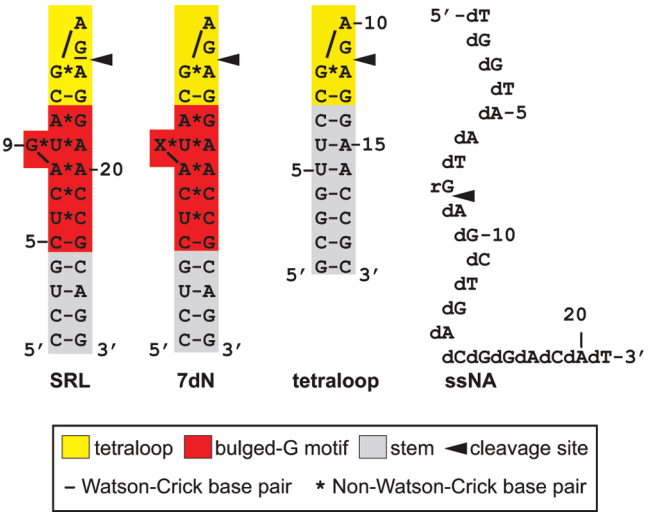

Figure 2. Substrates used in this study. The secondary structures of the SRL (reproducing nucleotides 4311−4337 of 28S rRNA from *Rattus norvegicus*), 7dN, tetraloop, and ssNA substrates with the tetraloops, bulged-G motifs, and stem structures highlighted in yellow, red, and gray, respectively. The 7dN substrate contains 7-deazaguanosine at the position labeled "X" within the bulged-G motif. The 2′OMe substrate (not shown) is the same as the SRL substrate, except that the underlined G has a methylated 2′-hydroxyl group to block site-specific cleavage.

detectable SRL cleavage, providing evidence that the bulged-G motif is an important element for SRL recognition.[17] It is unclear, however, whether this loss of activity arises from disruption of protein contact(s) to the bulged-G nucleobase or from indirect effects. Mutation of this bulged-G either destabilizes the motif because in the absence of SRL structural rearrangements neither an A, C, nor U mutation can replace the stabilizing contacts formed by the bulged-G nucleobase or changes the SRL structure to restore these stabilizing contacts. From the protein side of the enzyme−substrate interface, structural studies,[1,2] kinetic analyses of point mutants,[9] and similarity to the sequence and 3D structure of T1 nucleases have implicated active site residues H136 and E95 as the general acid and base, respectively.[9] Even though Y47, H49, and R120 are expected to stabilize the transition state,[9,18−20] their function is less well established. A nonsystematic survey of mutants identified two residues that affect specificity based on qualitative assays of cleavage of the SRL and/or the ribosome: Y47 and H49 in the active site.[19,21] A systematic deletion study, which again assayed cleavage qualitatively, indicated that the activity also depends on the lysine triad that is near but outside of the active site.[22]

As a prerequisite to determine the extent to which, and when during the reaction, each interface contact contributes to recognition, we previously established a kinetic framework for analysis of the reaction.[3,4] The reaction proceeds via two steps (Figure 1A). The first step, involving formation of an electrostatic complex (E:S), is monitored by K_m or the single turnover equivalent $K_{1/2}$, which are both equal to the K_D for binding of enzyme and substrate.[3,4] The second step, involving site recognition (hereafter designated docking) and RNA cleavage, is monitored by the catalytic constant k_{cat} (or the single turnover equivalent k_2). Restrictocin cleaves the SRL ∼1000-fold faster than a single-stranded RNA noncognate substrate, providing an empirical definition of the basal specificity.[3,4] Because formation

of the E:S complex is nonspecific,[3,4] specificity is achieved during the subsequent k_{cat} (or k_2) step.

Here, we exploited this kinetic framework to systematically investigate which contacts in the enzyme substrate interface contribute to specific recognition and determine the relative contribution that each makes to the specificity. This was done by constructing restrictocin point mutants that selectively disrupt interface contacts and comparing k_2 values for cleavage of the SRL substrate relative to a single-stranded substrate. To investigate which RNA structural elements contact protein interface residues, k_2 values were compared for restrictocin, or mutants thereof, cleaving variant substrates in which all or part of the SRL motifs have been removed. Our findings show that, as with other interfaces, only a subset of contacts contributes to specificity. One contact of this subset is critical, with the H49A mutation resulting in quantitative loss of specificity. Maximal catalytic activity occurs only when both SRL motifs are intact.

MATERIALS AND METHODS

Expression and Purification. Point mutants of restrictocin (D40A, K42A, Y47F, H49A, H49Q, F51A, T52A, R65A, K110A, K111A, K113A, K113R, K113Q, Q141A, D143A) were made with QuikChange (Stratagene) by using the pREST plasmid,[23] which contains the wild type (Wt) ribotoxin gene from *Aspergillus restrictus*, as the template. Wt and mutant restrictocin were recombinantly expressed, purified, and stored as described before.[4,23]

Construction of a Structural Model of the SRL−Restrictocin Complex. Even though this model has been previously cited (Figure 1B),[2] the details of how it was built were not described and therefore are presented here. Except for one nucleotide, the model was built from fragments of structures determined by X-ray crystallography and demonstrates that recognition of the bulged-G motif and site-specific cleavage can occur simultaneously. The largest fragment is from the "bound" structure[2] and includes coordinates for restrictocin and the SRL RNA, but excludes the GAGA tetraloop of this RNA. Coordinates for the first G and final A in the tetraloop are from the uncomplexed SRL structure[24] based on superposition with the bulged-G motif and stem from the bound structure. The uncomplexed structure is expected to reflect the ground state structure. Coordinates for the cleavage site nucleotide (second G of the tetraloop) were defined by superposition of restrictocin with the related RNase T1 structure, in which T1 was co-crystallized with a noncleavable dinucleotide substrate that shows how the target G docks in the active site.[25] Lastly, the A 5′ adjacent to the target G (the first A in the GAGA tetraloop) was modeled, followed by energy minimization to ensure reasonable stereochemistry.

RNA Substrates. Oligonucleotides, herein designated SRL, 7dN, tetraloop, and ssNA substrates (Figure 2) and the 2′-OMe substrate (Table 2), were synthesized either by Dharmacon, Inc. or at the University of Chicago. Three were purified by nondenaturing 20% 29:1 PAGE: the SRL substrate (5′-CCU GCU CAG UAC GAG AGG AAC CGC AGG), the 2′-OMe substrate (5′-CCU GCU CAG UAC GAX AGG AAC CGC AGG, where X is a 2′-methoxy substituted G), and the 7dN substrate (5′-CCU GCU CAX UAC GAG AGG AAC CGC AGG, where X is a 7-deazaguanosine nucleotide). The SRL substrate reproduces the nucleotides at positions 4311−4337 of 28S rRNA from *Rattus norvegicus*. The other two were purified by denaturing 20% 29:1 PAGE: the tetraloop substrate (5′-GCG GUU CCG AGA GGA ACC GC) and the ssNA (single-stranded nucleic acid) substrate (5′-d(TGGTAAT)-G-d(AGCTGACGGACAT)) designed to lack secondary structure.[26] Nondenaturing purification was used to remove a population of slow-cleaving RNA molecules from the substrate sample, which comigrates with the active substrates on denaturing PAGE.[4] These inactive species were not observed in tetraloop and ssNA substrates.

Kinetic Assays. Cleavage of the ^{32}P-labeled oligonucleotide substrate was performed as before[4] in 10 mM Tris (pH 7.5) containing 0.05% (v/v) Triton X-100 at 37 °C under k_2 conditions ($S_0 \ll K_{1/2} \ll E_0$) or under $k_2/K_{1/2}$ conditions ($S_0 \ll E_0 \ll K_{1/2}$). To avoid the use of rapid stopped flow quench kinetics and maintain the same measuring technique for all reactions studies, k_{cat} was measured instead of k_2 for the Wt enzyme and mutants with near Wt activity with $S_0 \gg K_m \gg E_0$. After initiating the reaction by rapid addition of 5′-[^{32}P]-labeled oligonucleotide substrates, 1.5 μL aliquots of the reaction were removed during a reaction time course and quenched by addition of 3.5 μL of stop solution (10 M urea containing 1% (w/v) SDS, 0.02% (w/v) xylene cyanol, and 0.04% (w/v) bromophenol blue). Samples were separated using 20% 29:1 PAGE containing 0.5 × TBE (45 mM Tris-borate (pH 8.3) and 1 mM EDTA) and 7 M urea. Samples were quantified using a PhosporImager (Molecular Dynamics). The time-dependent loss of substrate was fit to eq 1 using least-squares regression procedures in Origin (Microcal):

$$\text{FracS} = Ae^{-k_{obs}t} + y_0 \quad (1)$$

where FracS is the fraction of substrate, A is the cleavable fraction of the substrate, k_{obs} is the observed rate as defined in Figure 1A, t is time, and y_0 is the noncleavable fraction of the substrate. Under conditions of saturating enzyme ($E_o \gg K_{1/2}$) $k_{obs} = k_2$ and under conditions of saturating substrate ($S_o \gg K_{1/2}$) $k_{obs} = (k_2E_o)/K_{1/2}$. To ensure a reasonable fit, the sum of substrate fractions ($A + y_0$) was set to a value of 1.

We exploited the equivalence of k_{cat} and k_2[4] to efficiently measure rate constants for Wt and mutant enzymes. For Wt restrictocin, and mutants with near-Wt rates between 0.1 and ~1 s^{-1}, k_2 cannot be determined without the use of a rapid mixing and quenching techniques. On the other hand, these rate constants can be readily measured under k_{cat} conditions ($[S_0] \gg [E_0]$). Conversely, for mutants with slow cleavage rates (<~0.1 s^{-1}), k_{cat} cannot be readily measured due to the long time-points and high substrate concentrations required to observe cleavage. Thus, slow rates were determined under k_2 conditions ($[S_0] \ll [E_0]$).

Experimental Errors. Reported values represent the average and standard deviation of at least three measurements. All reported differences are statistically significant, with >90% confidence in a Student's t test.

RESULTS

Designs to Disrupt the Enzyme−Substrate Interface. To probe the protein side of the enzyme−substrate interface, we mutated 12 residues located at the crystallographically determined interface (Figure 1B, magenta surface). Protein backbone contributions were not evaluated (Figure 1A, blue surface). Of the 10 side chains that contact the RNA substrate (<3.4 Å), scanning alanine mutagenesis was performed on 9: K42A, H49A, T52A, R65A, K110A, K111A, K113A, Q141A, and D143A. For the 10th, we mutated Y47 to phenylalanine instead of alanine to

Table 1. Mutant Kinetic Parameters ($k_2/K_{1/2}$ (M^{-1} s^{-1}))[a]

restrictocin mutant	$k_2/K_{1/2}$ ($\times 10^8$ M^{-1} s^{-1})
wild-type	1.8 ± 0.7
D40A	0.6 ± 0.2
K42A	0.4 ± 0.1
Y47A	0.0002 ± 0.0001
Y47F	0.008 ± 0.002
H49A	0.0002 ± 0.0001
F51A	0.04 ± 0.02
T52A	0.4 ± 0.4
R65A	0.08 ± 0.02
K110A	0.006 ± 0.005
K111A	0.008 ± 0.003
K113A	0.0005 ± 0.0002
Q141A	4.2 ± 0.8
D143A	0.27 ± 0.04

[a] Reaction conditions: 10 mM Tris pH 7.5, 0.05% Triton X-100, 37 °C with E_0 = 1 nM, S_0 < 1 nM. Error values are standard deviation for three or more determinations.

disrupt a putative contact to the scissile phosphate (Figure 1C) while maintaining the capacity to form other active site contacts observed in the structure. The 11th mutant, D40A, is expected to disrupt binding of a potassium ion, which also contacts the SRL tetraloop.[2] The 12th mutant, F51A, is located in the active site pocket but does not contact the substrate (>3.4 Å). Mutations of other active site residues, which include R120, the putative general base, E95, and putative general acid, H136, were not analyzed herein because their contributions to catalysis have been characterized previously.[9,18−20,27−30]

To investigate the contribution of specific restrictocin−SRL contacts from the RNA side, variants that included multiple mutations were used rather than point mutants. The tetraloop and bulged G motif each form non-Watson Crick interactions.[12−16] Currently, it is impossible to predict how mutations in these motifs will affect the SRL structure. Thus, mutations of non-Watson−Crick interaction in either SRL motif were avoided to prevent unpredictable perturbations to the RNA structure. Four RNA variants were used. One is missing the putative N7 contact to the bulged-G (7dN substrate), a second is a hairpin containing the tetraloop motif but lacking the bulged-G motif (tetraloop substrate), and a third is an unstructured single-stranded nucleic acid (ssNA substrate) (Figure 2). The fourth one is the SRL with site-specific cleavage blocked by replacing the nucleophilic hydroxyl group with a methoxy group (2′-OMe substrate in Table 2; Materials and Methods).

Contacts Important for the Rate of SRL Cleavage by Restrictocin. To differentiate mutations that affect E:S stability from those that affect docking and cleavage, we determined ratios of Wt to mutant $k_2/K_{1/2}$ and k_2 (Materials and Methods; Tables 1 and 2). $K_{1/2}$ monitors nonspecific equilibrium association of E and S to form the E:S complex and k_2 monitors subsequent docking and cleavage (Figure 1A). Ratios of Wt to mutant k_2 values are designated by k_{rel} and the substrate used: k_{rel} (SRL), k_{rel} (ssNA), k_{rel} (7dN), and k_{rel} (tetraloop). Ratios based on $k_2/K_{1/2}$ are specifically indicated. The $k_2/K_{1/2}$ and k_2 ratios follow similar trends suggesting that changes to $k_2/K_{1/2}$ reflect k_2 contributions to docking and cleavage, not to formation of the E:S complex (Figure 3A, compare gray bars to open bars). Therefore, only k_2 ratios will be discussed hereafter.

The k_{rel} (SRL) values for restrictocin mutants (Table 1 and Figure 3) range from a high of 2190 ± 150 to a low of 1 (Figure 3A), indicating that the surface residues contribute differentially to k_2 and therefore affect either substrate docking, activity or both. Mutation of four contact residues (D40A, K42A, T52A, and Q141A) located at the periphery of the interface had k_{rel} (SRL) < 10, reflecting small energy differences of less than 1.4 kcal mol^{-1}. Evidently, these disrupted contacts make minor contributions to substrate docking and activity. The remaining eight mutations (Y47F, H49A, F51A, R65A, K110A, K111A, K113A, and D143A) have k_{rel} (SRL) ≥ 10 and cluster along the RNA helical axis of the enzyme−substrate interface.

The largest effects, k_{rel} (SRL) > 1000, are seen with H49A and K113A. The effect of the K113A mutation is in accord with structural studies[2] showing that this lysine residue forms sequence-specific interactions with the SRL by contacting N7 and O6 of the bulged G (Figure 1D). To assess the contributions of either hydrogen bonding or salt bridge interactions made by the K113 amino group, two mutants were made. Mutation to K113R partially restores k_2, whereas K113Q offers no restoration, with a k_{rel} (SRL) > 1000 like K113A. These results provide evidence that the positive charge at residue 113 contributes to this interface contact.

Unlike K113, H49 is in the active site and based on kinetic studies[9] is expected to contribute to transition state stabilization. This contribution may arise from charge neutralization of the transition state by H49, which is expected to carry partial positive charge under the reaction conditions based upon the pK_a value of 7.7 ± 0.2 measured for the free enzyme[29] (substrate binding is expected to perturb the pK_a further). Also, the imidizoyl moiety of H49 contacts the oxygen atom of the nucleophilic 2′ hydroxyl group in the structural model (Figure 1B)[2] and in the structure of RNase T1 bound to a substrate analogue.[2,25] This contact may help nucleophilic activation by the putative general base (E95). The H49Q mutation, expected to maintain hydrogen-bonding capabilities, restores only 16-fold of the 2190-fold k_2 loss for k_{rel} (SRL) observed for the H49A mutant. The remaining 131 ± 66 fold for k_{rel} (SRL) of H49Q may arise from the loss of electrostatic catalysis provided by the partial charge of H49 contributing to electrostatic catalysis[29,31] or from other factors.

Y47F and K111A showed noteworthy effects with k_{rel} (SRL) values of 280 ± 60 and 110 ± 20, respectively. On the basis of mutational[21] and crystallographic studies[2] (Figure 1C), the active site residue Y47 contributes to transition state stabilization. We examined Y47F to test the contribution of the putative contact between its hydroxyl group and the scissile phosphate (Figure 1C). Positioned outside but near the active site, K111 is observed to contact the phosphodiester backbone of the bulged-G motif (Figure 1D), in contrast to K113, which contacts the bulged-G nucleobase. Loss of activity for mutants of these residues suggests that the hydroxyl group of Y47 and the backbone contacts made by K111 contribute to site-specific cleavage.

Four mutants, R65A, F51A, K110A, and D143A, had a smaller effect on k_{rel} (SRL), with ratios between 10 and 100. F51 is located in the pocket for binding the target nucleobase but does not contact the substrate; perhaps mutation of this residue affects k_2 values by perturbing the active site structure. R65 is expected to form a salt bridge to a phosphate group in the SRL tetraloop; the loss of activity when removing this contact implies that contacts to the tetraloop contribute to SRL recognition (see the k_{rel} (tetraloop) data below). D143 lies at the edge of the SRL

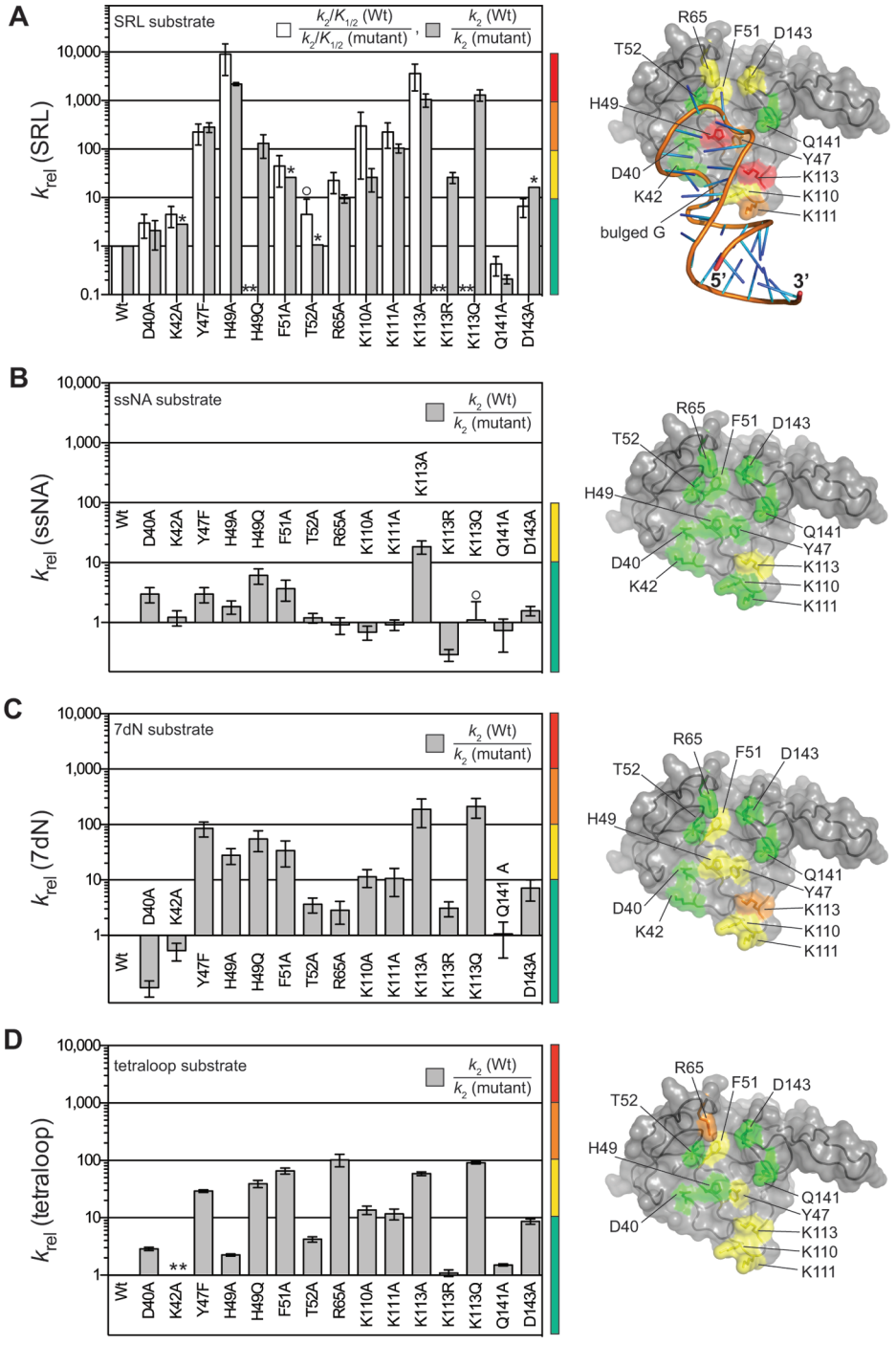

Figure 3. Effect of restrictocin mutations on cleavage of the SRL (A), ssNA (B), 7dN (C), and tetraloop (D) substrates. For each substrate the k_{rel} (k_2 (Wt)/k_2 (mutant)) is shown for each protein mutant (gray bars) and color-coded onto the protein surface (right) with k_{rel} > 1000 (red), k_{rel} between 100 and 1000 (orange), k_{rel} between 10 and 100 (yellow) and k_{rel} < 10 (green). For the SRL substrate, white bars are k_{rel} for the ratios $k_2K_{1/2}$ (Wt) / $k_2K_{1/2}$ (mutant). Due to the lack of structural data docked models of restrictocin in complex with the 7dN, ssNA and tetraloop substrates are not presented. Error bars represent propagated error from the calculation of each ratio using data in Tables 1 and 2. Asterisks mark k_2 SRL measurements made only once, double asterisks indicate measurements that were not determined, and circles mark bars for which only upward errors are drawn because the downward error extends to negative values, which are undefined on a log scale.

tetraloop binding site and may therefore contribute directly or indirectly to SRL recognition. Like K111 and K113, K110 contacts to the bulged-G motif (Figure 1D) contribute to recognition.

Differential Roles of Contacts That Contribute to Specificity and Basal Activity. The k_{rel} (SRL) data in Figure 3A do not differentiate between effects on specificity and on basal endoribonuclease activity. The latter does not contribute to specificity because loss of basal activity indiscriminately slows cleavage of all substrates. Because the initial binding step between restrictocin and the SRL substrate is nonspecific,[3,4] specificity is defined herein as the ratio of

dx.doi.org/10.1021/bi1018336 |*Biochemistry* 2011, 50, 3004–3013

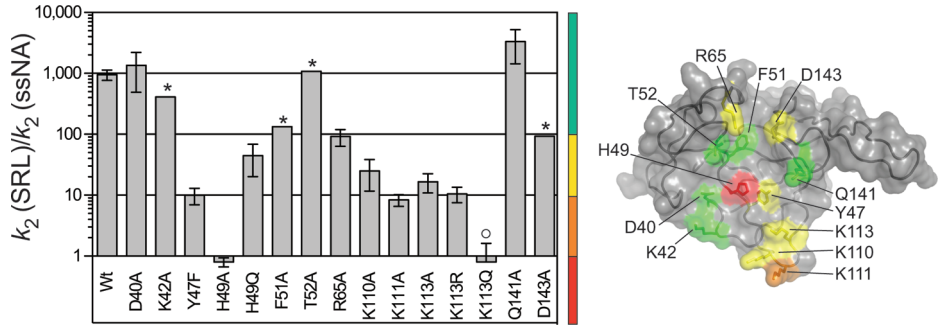

Figure 4. Effect of restrictocin mutation on SRL specificity. Specificity is defined as the ratio k_2 (SRL)/k_2 (ssNA) with values >100 (green), from 10 to 100 (yellow), from 1 to 10 (orange), and from 0 to 1 (red). Error bars and markings are as in Figure 3.

k_2 for specific SRL cleavage vs cleavage of the unstructured ssNA substrate. Basal activity is defined as cleavage of a substrate mimic that shares the same rate-limiting step as cleavage of the SRL substrate but lacks site-specific recognition opportunities. Cleavage of the ssNA substrate by restrictocin approximates basal activity because this substrate satisfies five design criteria. First, it is 21-nucleotides long to ensure that the stability of its initial nonspecific electrostatic E:S complex (Figure 1A, step 1) is indistinguishable from that of the SRL substrate.[3,4] Second, to simplify cleavage rate measurements we made a single cleavage site by including only one ribonucleotide. Third, the scissile phosphate is flanked on both sides by single-stranded deoxynucleotides to disrupt contacts that recognize features of a specific SRL fold. Fourth, the scissile phosphate of both the ssNA and SRL substrates are flanked by G and A bases to permit them to dock in a similar manner when bound to restrictocin. Fifth, a related single-stranded RNA substrate and the SRL substrate have similar pH−rate profiles, suggesting that these substrates have the same rate-limiting step, and the k_2 values for restrictocin cleavage of the ssNA and ssRNA substrates are identical.[26] Therefore, we infer that the ssNA and SRL substrates have the same rate-limiting step.

Under our assay conditions, k_2 for ssNA is ∼1000 smaller than k_2 for the SRL substrate but still ∼1 million fold larger than the rate constant for the uncatalyzed reaction (estimated using equation *e* from ref 32). Assuming a single mode of docking as shown in Figure 1C, catalytic residues like Y47 and H49, which do not make sequence specific contacts, would be expected to affect both basal activity and specific cleavage. To test whether the k_{rel} (SRL) effects are due to loss of basal activity we determined k_2 for each mutant using the ssNA substrate.

Mutation of active site residues has only minor effects on basal activity, k_{rel} (ssNA) < 10 (Table 1 and Figure 3B). Similar results were observed for the other mutants, except for K113A, which had a slightly larger value of 18 ± 5. Mutation of K113 to either arginine or glutamine attenuates this effect (reducing it to <10). Perhaps K113 assists in the docking of both the SRL and nonspecific substrates, whereas K113R and K113Q assist in the docking of only the SRL substrate.

Quantitation of Cleavage Specificity. To directly investigate contributions of each interface contact to specificity, we determined for each mutant the k_2 ratio for cleavage of the SRL RNA and the nonspecific ssNA substrate (Figure 4). Only one alanine mutation abolishes specificity by dropping this k_2 ratio by over 1000-fold from 955 to 0.8 (H49A). Y47F, K110A, K111A, and K113A also show notable effects, reducing specificity by 96-, 38-, 115-, and 57-fold, respectively. Smaller effects, within ∼10-fold of the k_2 Wt ratio, are observed for D40A, K42A, F51A, T52A, R65A, Q141A, and D143A.

The observation that the active site mutants Y47F and H49A greatly reduce SRL cleavage (Figure 4) without affecting basal activity (k_{rel} (ssNA) < 10 and Table 2 and Figure 3B) indicates that Y47 and H49 participate in SRL cleavage but not the ssNA cleavage. The finding that the SRL substrate, but not the ssNA substrate, engages Y47 and H49 in the cleavage mechanism implies that these substrates dock differently into the active site (Figure 5).

To investigate the contribution of interface residues to cleavage fidelity (the preference for cleavage at the correct site versus other sites within the SRL), we monitored the rate of cleavage for the 2′-OMe substrate methylated to block cleavage at the correct site but permit cleavage at other sites within the SRL (Figure 2). For the four mutants tested (D40A, K110A, K111A, and K113A; Table 2), the average rate of miscleavage (overall k_2 divided by the number of miscleavage sites within the methylated SRL substrate) was comparable (<10-fold difference) to k_2 for the ssNA substrate. These results suggest that the same restrictocin residues that contribute to SRL cleavage specificity also contribute to cleavage fidelity and that in the context of the SRL structure restrictocin residues impart their maximal catalytic contributions only during cleavage at the correct site. Like the ssNA substrate, the 2′-OMe substrate does not fully engage the catalytic machinery, supporting the notion that the enzyme−substrate complex populates a distinct nonspecific docking mode during miscleavage. In subsequent experiments, we investigated how the bulged-G motif contributes to specificity by determining k_{rel} for the substrates that either partially or completely removed the bulged-G motif (7dN and tetraloop substrates, respectively) and compared these values to k_{rel} (SRL).

Recognition of the Bulged-G Motif by Restrictocin. In the structural model (Figure 1D), K113 resides within hydrogen bonding distance of the N7 and O7 atoms of the bulged-G nucleobase in the eponymous motif. To probe recognition of this nucleobase, we disrupted the contact between K113 and N7 by using the 7dN substrate in which the bulged-G nucleobase is replaced by a 7-deazaguanosine (Figure 2). This single-atom substitution is nondisruptive of the SRL fold[16] and thus offers an appealing way to test the importance of N7 contacts. The 7dN modification reduces k_2 ∼ 60-fold for wild-type restrictocin, eliminating a large fraction of the ∼1000-fold specificity. This finding implies that interaction with N7 of the bulged-G by restrictocin contributes to catalysis and specificity, in accord with the structural model (Figure 1D).

Table 2. Comparison of Catalytic Constants (k_{cat} or k_2 (s^{-1})) for Various Substrates[a]

restrictocin	SRL	ssNA	2′-OMe[b]	7dN	tetraloop
wild-type	1.05 ± 0.07	0.0011 ± 0.0002	0.0003 ± 0.0001	0.017 ± 0.005	0.0164 ± 0.0001
D40A	0.5 ± 0.3	0.00037 ± 0.00008	0.00015 ± 0.00002	0.15 ± 0.02	0.0057 ± 0.0004
K42A	0.37	0.0009 ± 0.0002	n.d.[c]	0.032 ± 0.006	n.d.[c]
Y47F	0.0037 ± 0.0008	0.00037 ± 0.00008	n.d.[c]	0.00020 ± 0.00001	0.00056 ± 0.00003
H49A	0.00048 ± 0.00001	0.0006 ± 0.0001	n.d.[c]	0.00061 ± 0.00008	0.0073 ± 0.0003
H49Q	0.008 ± 0.004	0.00018 ± 0.00004	n.d.[c]	0.00031 ± 0.00009	0.00042 ± 0.00006
F51A	0.04	0.0003 ± 0.0001	n.d.[c]	0.0005 ± 0.0002	0.00025 ± 0.00003
T52A	0.99	0.00092 ± 0.00002	n.d.[c]	0.0047 ± 0.0003	0.0039 ± 0.0004
R65A	0.11 ± 0.02	0.0012 ± 0.0003	n.d.[c]	0.006 ± 0.002	0.00016 ± 0.00004
K110A	0.04 ± 0.02	0.0016 ± 0.0003	0.0008 ± 0.0006	0.0015 ± 0.0003	0.0012 ± 0.0002
K111A	0.010 ± 0.002	0.0012 ± 0.0001	0.0012 ± 0.0006	0.0016 ± 0.0007	0.0014 ± 0.0003
K113A	0.0010 ± 0.0003	0.00006 ± 0.00001	0.00007 ± 0.00002	0.00009 ± 0.00004	0.00028 ± 0.00002
K113R	0.04 ± 0.01	0.0038 ± 0.0005	n.d.[c]	0.0055 ± 0.0003	0.015 ± 0.002
K113Q	0.0008 ± 0.0002	0.001 ± 0.001	n.d.[c]	0.00008 ± 0.00002	0.000180 ± 0.000009
Q141A	5 ± 1	0.0015 ± 0.0008	n.d.[c]	0.016 ± 0.009	0.0109 ± 0.0005
D143A	0.065	0.00070 ± 0.00001	n.d.[c]	0.0024 ± 0.0007	0.0019 ± 0.0002

[a] Reaction conditions and error values are the same as in Table 1. k_{cat} was measured under multiple turnover conditions for values >0.1 s^{-1}. k_2 was measured under single turnover conditions for values <0.1 s^{-1}. Error values are standard deviation for three or more determinations; for entries without error values only one measurement was made. [b] Values for 2′OMe substrate represent average rate of all miscleavages. [c] Not determined.

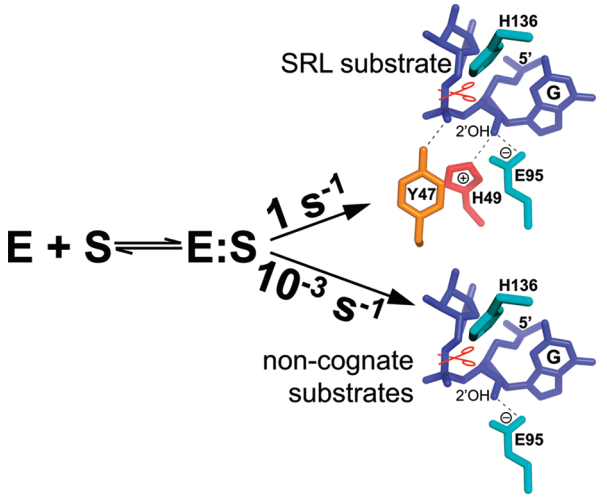

Figure 5. The mode of substrate docking determines its cleavage rate. All nucleic acid substrates (S) with a length greater than about 20 nucleotides bind to restrictocin (E) with similar affinities and form an electrostatic complex, E:S. Specificity is conferred by subsequent docking into the active site. The cognate SRL substrate docks in a manner that fully engages all the active site residues, thereby achieving a k_2 of ~1 s^{-1} (upper right panel). In contrast, noncognate substrates dock in a less productive manner (lower right panel) that fails to engage some active site residues and thus react ~1000-fold more slowly.

We also determined the contribution of individual restrictocin residues to recognition of the 7dN substrate (Table 1 and Figure 3C). The k_{rel} (7dN) ratios range from a high of ~190 to a low of 1. Six of the mutations show a minor effect (k_{rel} (7dN) < 10): D40A, K42A, T52A, R65A, Q141A, and D143A. Five mutations showed larger effects (k_{rel} (7dN) > 10). Three of these (Y47F, H49A, and F51A) are in the active site, whereas the remaining two (K110A and K111A) contact the bulged-G motif (Figure 1C,D). The largest change, k_{rel} (7dN) > 100, was observed for K113A, which is unable to contact either O6 or N7 of a bulged-G nucleobase. The N7, not the O6, contact is expected to be disrupted by the deaza modification of this substrate variant. To assess the role of hydrogen bonding and salt bridge contacts in SRL recognition by K113, the arginine and glutamine mutants were tested. The K113R mutant restores k_2 activity to within ~3-fold of the Wt level, whereas the K113Q does not. These results provide evidence that electrostatic interactions between the cationic K113 and the anionic RNA backbone contribute to the docking and catalytic step (k_2). Apparently, K113 is involved in both hydrogen binding and electrostatic interactions with the SRL substrate.

Tetraloop Recognition by Restrictocin. Our previous studies showed that the tetraloop substrate is cleaved specifically.[4] To identify restrictocin contacts that contribute to tetraloop recognition, we determined k_{rel} (tetraloop) (Table 1 and Figure 3D). Like the 7dN substrate, the tetraloop substrate is cleaved ~60-fold more slowly than the SRL by Wt restrictocin. Five mutants (D40A, H49A, T52A, Q141A, and D143A) had only minor effects on activity (k_{rel} (tetraloop) < 10), indicating that these side chains do not make notable contributions to tetraloop recognition in the absence of the bulged-G motif. The remaining six mutants had k_{rel} (tetraloop) >10-fold: Y47F, F51A, R65A, K110A, K111A, and K113A. With the exception of R65A, these mutants also had reduced activity on the 7dN substrate. Interestingly, R65 contributes more to recognition of the tetraloop substrate than it contributes to recognition of the SRL substrate: the R65A mutant has the largest k_{rel} (tetraloop), with a value of 103 ± 26 (Figure 3D), whereas its k_{rel} (SRL) is only 9.5 ± 1.8. Moreover, the R65A mutant has a k_2 ratio for cleavage of the SRL RNA vs the nonspecific ssNA substrate that is ~10-fold less than this ratio for Wt enzyme (Table 2 and Figure 4).

Loss of tetraloop substrate activity for the K110A, K111A, and K113A mutants was unexpected because these mutations delete putative contacts to the bulged-G motif, which has been removed from the tetraloop substrate. A plausible explanation arises from a

simple modeling study (data not shown) that replaces the bulged-G motif with an A-form stem structure. In the model, the trajectory of the phosphate backbone of the A-form stem structure in the tetraloop substrate approaches close enough to form electrostatic interactions with K110, K111, and K113. To further test the contribution of K113, k_{rel} (tetraloop) values were determined for the arginine and glutamine mutants. K113R restores tetraloop substrate activity to Wt levels, whereas K113Q does not. These findings offer evidence that K113, and perhaps K110 and K111 as well, contribute to docking via electrostatic interactions to the WC stem of the tetraloop substrate.

Interestingly, H49A shows no k_{rel} (tetraloop) effect (Figure 3D), whereas it shows a medium effect for k_{rel} (7dN) (Figure 3C) and large effects for both k_{rel} (SRL) (Figure 3A) and specificity (Figure 4). An H49 contribution to k_2 for reactions with the SRL and the 7dN substrates, but not with the tetraloop and ssNA substrates, suggests that bulged-G motif recognition is required to engage H49 in catalysis. Thus, our findings show that although contacts to the tetraloop are sufficient to produce specific cleavage, maximal cleavage rates and specificity are observed only when the enzyme contacts both SRL motifs: the bulged-G motif and tetraloop.

DISCUSSION

The findings reported here systematically probe ribotoxin residues and the extent to which each one contributes to substrate recognition. Scanning mutagenesis reveals that of the 12 residues predicted to lie within the RNA−protein interface, only 7 contribute to activity (Tables 1 and 2; Figures 3 and 4). Of these, only mutation of the active site H49 (Figure 1C) completely abolishes the specificity of restrictocin by reducing its rate of cleavage to that of the nonspecific ssNA substrate (Figure 4). Four other residues make notable contributions to enzyme recognition of the SRL RNA. Y47 is in the active site. In contrast, the other three residues (K110, K111, and K113) are located outside of the active site and recognize the bulged-G motif. As with two other well-studied RNA−protein interfaces, the signal recognition particle and MS2 coat protein,[33,34] only a small subset of the interface contacts, often designated "hot spots", contribute to recognition. The view emerging from these studies and studies of protein−protein interfaces[35] is that hot spots are a common feature of macromolecular recognition. Because, at present, in silico calculations cannot reliably identify hot spots, our quantitative and systematic investigations of an RNA−protein interface may be used to develop better computational approaches.[36]

To cleave the SRL ∼1000-fold faster than a single-stranded nucleic acid substrate, ssNA, restrictocin recognizes its substrate not during the first but rather the second kinetic step of the reaction, k_2, which involves site-docking and cleavage (Figure 1A).[3,4] The importance of SRL motifs to docking was probed by comparing k_2 values for restrictocin or its mutants cleaving SRL variants with one or both motifs missing. Removal of the bulged-G motif from the SRL substrate results in a 64-fold loss in activity with an additional 15-fold loss upon complete removal of secondary structure (absence of the bulged-G motif, tetraloop, and stem structure). These findings indicate that the majority of the contribution to specificity arises from contacts to the bulged-G motif, in the context of the SRL, in accord with previous studies.[3,17,37] The data in Figure 3 indicate that the lysine triad (K110, K111, and K113) and in particular K113 contributes to bulged-G recognition. Our 7dN data and mutational data of others[22] show that each residue in the lysine triad is needed for full activity. Given the juxtaposition of these side chains, it is reasonable to expect that mutating one would affect positioning of the other two (Figure 1D). Even though bulged-G motif recognition contributes to catalysis, recognition relies as well on additional tetraloop contacts to active site residues.

Previous qualitative studies indicated the importance of Y47 and H49 to specificity.[19,21] Here, our kinetic analysis provides insight into the molecular basis of the linkage between the mode of substrate docking and catalysis with different substrates engaging active site residues Y47 and H49 to different degrees. Structural and functional studies[2,9] provide evidence that the active site histidine (H49) does not make sequence specific contacts to the substrate (Figure 1C). Rather, it contributes to transition state stabilization and is expected to contact the nucleophilic 2′ hydroxyl group (Figure 1C). If all nucleic acid substrates docked similarly, mutation of H49 would have affected the activity of every substrate to a similar extent. Our kinetic studies do not support this model. Restrictocin cleaves the ssNA substrate with no detectable contribution from the active site residues Y47 and H49 (Figure 3B). In contrast, this enzyme cleaves the tetraloop substrate by engaging Y47 but not H49 (Figure 3D) and cleaves the SRL and 7dN substrates with participation of both active site residues (Figure 3C). These substrate-dependent contributions of active site residues to catalysis likely reflect different modes of docking for cognate and noncognate substrates (Tables 1 and 2 and Figures 3 and 4). Evidently, bulged-G recognition is needed to engage H49, whereas the tetraloop by itself appears sufficient to engage Y47.

The simplest model to account for the Y47F and H49A data involves at least two modes of substrate docking into the active site (Figure 5). In the nonspecific mode, docking of non-SRL substrates permits only partial engagement of the catalytic residues and results in an impaired cleavage rate. In contrast, docking in the specific mode with the SRL enables full engagement of the catalytic machinery (including Y47 and H49) to achieve a ∼1000-fold rate enhancement of site-cleavage of the SRL relative to cleavage of ssNA substrates.

The molecular basis by which different substrates elicits two docking modes is unknown, but two attractive candidate mechanisms exist. In the first, active site docking of the SRL places its nucleophile and scissile bond in position close enough to engage the side chains of Y47 and H49. For docking of non-SRL substrates, these side chains are farther away from the nucleophile and scissile bond because only the SRL possesses the contacts necessary to stabilize the specific docking mode. Hence, the nonspecific docking mode results in slower cleavage rates. In the second mechanism, only SRL docking triggers an induced fit in the RNA, protein or both to shorten the distance and thereby engage Y47 and H49 catalytically.

The two modes of docking with differential activity create a kinetic discrimination mechanism to ensure that the SRL is cleaved faster than non-SRL substrates. This mechanism of active site docking for the SRL substrate offers functional support for the structural model of site docking (Figure 1C,D and the upper right panel of Figure 5) in which both SRL motifs are simultaneously recognized. As a result, the target nucleotide is positioned in a base-flipped form to orient it for maximal activity.

Recognition of RNA by restrictocin exemplifies two recurrent themes in RNA−protein recognition.[38] Groove binding is

illustrated by the lysine triad loop recognizing the enlarged major groove of the SRL and its distinctive bulged-G nucleobase. β-Sheet binding is illustrated by the unfolded tetraloop that docks into the active site pocket. Our work shows that restrictocin couples these recognition strategies to achieve specificity.

AUTHOR INFORMATION

Corresponding Author

*(C.C.C.) Telephone: (847) 578-8611. Fax: (847) 578-3240. E-mail: carl.correll@rosalindfranklin.edu. (J.A.P.) Phone (773) 702-9312. Fax: (773) 702-0439. E-mail: jpicciri@uchicago.edu.

Present Addresses

[||]Department of Biochemistry and Molecular Biology, Rosalind Franklin University of Medicine & Science.

[#]Department of Biochemistry and Biophysics, University of California, San Francisco, CA 94158.

[▽]Department of Laboratory Oncology Research, Curtis and Elizabeth Anderson Cancer Institute, Memorial Health University Medical Center, Savannah, GA 31404.

Funding Sources

This work was supported by grants to C.C.C. from the National Institutes of Health (GM59872 and GM070491) and to J.A.P. from Howard Hughes Medical Institute.

ACKNOWLEDGMENT

We are grateful to Y.-L. Chan, J. Olvera, and I. G. Wool for valuable advice and discussion and to N. Gao for technical assistance.

ABBREVIATIONS USED

SRL, sarcin/ricin loop; Wt, wild type; E:S, electrostatic Michaelis complex; tetraloop substrate, SRL in which bulged-G motif is replaced with Watson−Crick stem; 7dN substrate, SRL in which the bulged-G contains a 7 deazaguanosine; ssNA substrate, oligonucleotide with a single riboguanosine embedded in single-stranded DNA

REFERENCES

(1) Yang, X., and Moffat, K. (1996) Insights into specificity of cleavage and mechanism of cell entry from the crystal structure of the highly specific *Aspergillus* ribotoxin, restrictocin. *Structure 4*, 837–852.

(2) Yang, X., Gerczei, T., Glover, L., and Correll, C. C. (2001) Crystal structures of restrictocin-inhibitor complexes with implications for RNA recognition and base flipping. *Nat. Struct. Biol. 8*, 968–973.

(3) Korennykh, A. V., Piccirilli, J. A., and Correll, C. C. (2006) The electrostatic character of the ribosomal surface enables extraordinarily rapid target location by ribotoxins. *Nat. Struct. Mol. Biol. 13*, 436–443.

(4) Korennykh, A. V., Plantinga, M. J., Correll, C. C., and Piccirilli, J. A. (2007) Linkage between substrate recognition and catalysis during cleavage of sarcin/ricin loop RNA by restrictocin. *Biochemistry 46*, 12744–12756.

(5) Voorhees, R. M., Schmeing, T. M., and Ramakrishnan, V. (2010) The mechanism of action of GTP hydrolysis on the ribosome. *Science 330*, 835–838.

(6) Lacadena, J., Alvarez-Garcia, E., Carreras-Sangra, N., Herrero-Galan, E., Alegre-Cebollada, J., Garcia-Ortega, L., Onaderra, M., Gavilanes, J. G., and Martinez Del Pozo, A. (2007) Fungal ribotoxins: molecular dissection of a family of natural killers. *FEMS Microbiol. Rev. 31* (2), 212–237.

(7) Wool, I. G. (1997) *Structure and Mechanism of Action of the Cytotoxic Ribonuclease α-Sarcin*, Academic Press, Inc., San Diego.

(8) Sacco, G., Drickamer, K., and Wool, I. G. (1983) The primary structure of the cytotoxin alpha-sarcin. *J. Biol. Chem. 258*, 5811–5818.

(9) Lacadena, J., Martinez del Pozo, A., Martinez-Ruiz, A., Perez-Canadillas, J. M., Bruix, M., Mancheno, J. M., Onaderra, M., and Gavilanes, J. G. (1999) Role of histidine-50, glutamic acid-96, and histidine-137 in the ribonucleolytic mechanism of the ribotoxin alpha-sarcin. *Proteins 37*, 474–484.

(10) Munishkin, A., and Wool, I. G. (1997) The ribosome-in-pieces: binding of elongation factor EF-G to oligoribonucleotides that mimic the sarcin/ricin and thiostrepton domains of 23S ribosomal RNA. *Proc. Natl. Acad. Sci. U.S.A. 94*, 12280–12284.

(11) Endo, Y., Chan, Y. L., Lin, A., Tsurugi, K., and Wool, I. G. (1988) The cytotoxins alpha-sarcin and ricin retain their specificity when tested on a synthetic oligoribonucleotide (35-mer) that mimics a region of 28 S ribosomal ribonucleic acid. *J. Biol. Chem. 263*, 7917–7920.

(12) Szewczak, A. A., and Moore, P. B. (1995) The sarcin/ricin loop, a modular RNA. *J. Mol. Biol. 247*, 81–98.

(13) Szewczak, A. A., Moore, P. B., Chan, Y. L., and Wool, I. G. (1993) The conformation of the sarcin/ricin loop from 28S ribosomal RNA. *Proc. Natl. Acad. Sci. U.S.A. 90*, 9581–9585.

(14) Ban, N., Nissen, P., Hansen, J., Moore, P. B., and Steitz, T. A. (2000) The complete atomic structure of the large ribosomal subunit at 2.4 Å resolution. *Science 289*, 905–920.

(15) Correll, C. C., and Swinger, K. (2003) Common and distinctive features of GNRA tetraloops based on a GUAA tetraloop structure at 1.4 Å resolution. *RNA 9*, 355–363.

(16) Correll, C. C., Beneken, J., Plantinga, M. J., Lubbers, M., and Chan, Y. L. (2003) The common and the distinctive features of the bulged-G motif based on a 1.04 A resolution RNA structure. *Nucleic Acids Res. 31*, 6806–6818.

(17) Gluck, A., and Wool, I. G. (1996) Determination of the 28 S ribosomal RNA identity element (G4319) for alpha-sarcin and the relationship of recognition to the selection of the catalytic site. *J. Mol. Biol. 256*, 838–848.

(18) Kao, R., Shea, J. E., Davies, J., and Holden, D. W. (1998) Probing the active site of mitogillin, a fungal ribotoxin. *Mol. Microbiol. 29*, 1019–1027.

(19) Nayak, S. K., Bagga, S., Gaur, D., Nair, D. T., Salunke, D. M., and Batra, J. K. (2001) Mechanism of specific target recognition and RNA hydrolysis by ribonucleolytic toxin restrictocin. *Biochemistry 40*, 9115–9124.

(20) Masip, M., Lacadena, J., Mancheno, J. M., Onaderra, M., Martinez-Ruiz, A., del Pozo, A. M., and Gavilanes, J. G. (2001) Arginine 121 is a crucial residue for the specific cytotoxic activity of the ribotoxin alpha-sarcin. *Eur. J. Biochem. 268*, 6190–6196.

(21) Alvarez-Garcia, E., Garcia-Ortega, L., Verdun, Y., Bruix, M., Martinez del Pozo, A., and Gavilanes, J. G. (2006) Tyr-48, a conserved residue in ribotoxins, is involved in the RNA-degrading activity of alpha-sarcin. *Biol. Chem. 387*, 535–541.

(22) Gluck, A., and Wool, I. G. (2002) Analysis by systematic deletion of amino acids of the action of the ribotoxin restrictocin. *Biochim. Biophys. Acta 1594*, 115–126.

(23) Plantinga, M. J., Korennykh, A. V., Piccirilli, J. A., and Correll, C. C. (2008) Electrostatic interactions guide the active site face of a structure-specific ribonuclease to its RNA substrate. *Biochemistry 47*, 8912–8918.

(24) Correll, C. C., Wool, I. G., and Munishkin, A. (1999) The two faces of the *Escherichia coli* 23 S rRNA sarcin/ricin domain: The structure at 1.11 Å resolution. *J. Mol. Biol. 292*, 275–287.

(25) Arni, R. K., Watanabe, L., Ward, R. J., Kreitman, R. J., Kumar, K., and Walz, F. G. (1999) Three-dimensional structure of ribonuclease T1 complexed with an isosteric phosphonate substrate analogue of GpU: alternate substrate binding modes and catalysis. *Biochemistry 38*, 2452–2461.

(26) Korennyhk, A. V. (2005) Recognition of the sarcin/ricin loop RNA and of the ribosome by ribosome-inactivating proteins, in *Department of Chemistry*, The University of Chicago, Chicago.

(27) Yang, R., and Kenealy, W. R. (1992) Effects of amino-terminal extensions and specific mutations on the activity of restrictocin. *J. Biol. Chem. 267*, 16801–16805.

(28) Lacadena, J., Mancheno, J. M., Martinezruiz, A., Delpozo, A. M., Gasset, M., Onaderra, M., and Gavilanes, J. G. (1995) Substitution of histidine-137 by glutamine abolishes the catalytic activity of the ribosome-inactivating protein alpha-sarcin. *Biochem. J. 309*, 581–586.

(29) Perez-Canadillas, J. M., Campos-Olivas, R., Lacadena, J., Martinez del Pozo, A., Gavilanes, J. G., Santoro, J., Rico, M., and Bruix, M. (1998) Characterization of pKa values and titration shifts in the cytotoxic ribonuclease alpha-sarcin by NMR. Relationship between electrostatic interactions, structure, and catalytic function. *Biochemistry 37*, 15865–15876.

(30) Garcia-Mayoral, M. F., Perez-Canadillas, J. M., Santoro, J., Ibarra-Molero, B., Sanchez-Ruiz, J. M., Lacadena, J., del Pozo, L. M., Gavilanes, J. G., Rico, M., and Bruix, M. (2003) Dissecting structural and electrostatic interactions of charged groups in alpha-sarcin. An NMR study of some mutants involving the catalytic residues. *Biochemistry 42*, 13122–13133.

(31) Perez-Canadillas, J. M., Garcia-Mayoral, M. F., Laurents, D. V., Martinez del Pozo, A., Gavilanes, J. G., Rico, M., and Bruix, M. (2003) Tautomeric state of alpha-sarcin histidines. Ndelta tautomers are a common feature in the active site of extracellular microbial ribonucleases. *FEBS Lett. 534*, 197–201.

(32) Li, Y., and Breaker, R. R. (1999) Kinectics of RNA degradation by specific base catalysis of transesterification involving the 2′-hydoxyl group. *J. Am. Chem. Soc. 121*, 5364–5372.

(33) Batey, R. T., Sagar, M. B., and Doudna, J. A. (2001) Structural and energetic analysis of RNA recognition by a universally conserved protein from the signal recognition particle. *J. Mol. Biol. 307*, 229–246.

(34) Hobson, D., and Uhlenbeck, O. C. (2006) Alanine scanning of MS2 coat protein reveals protein-phosphate contacts involved in thermodynamic hot spots. *J. Mol. Biol. 356*, 613–624.

(35) Ofran, Y., and Rost, B. (2007) Protein-protein interaction hotspots carved into sequences. *PLoS Comput. Biol. 3*, e119.

(36) Perez-Cano, L., and Fernandez-Recio, J. Optimal protein-RNA area, OPRA: a propensity-based method to identify RNA-binding sites on proteins, *Proteins 78*, 25−35.

(37) Korennykh, A. V., Correll, C. C., and Piccirilli, J. A. (2007) Evidence for the importance of electrostatics in the function of two distinct families of ribosome inactivating toxins. *RNA (New York, N.Y.) 13*, 1391–1396.

(38) Draper, D. E. (1999) Themes in RNA-protein recognition. *J. Mol. Biol. 293*, 255–270.